

# Critical cluster size and droplet nucleation rate from growth and decay simulations of Lennard-Jones clusters

Hanna Vehkamäki<sup>a)</sup> and Ian J. Ford

*Department of Physics and Astronomy, University College London, Gower Street, London WC1E 6BT, United Kingdom*

(Received 22 July 1999; accepted 6 December 1999)

We study a single cluster of Lennard-Jones atoms using a novel and physically transparent Monte Carlo simulation technique. We compute the canonical ensemble averages of the grand canonical growth and decay probabilities of the cluster, and identify the critical cluster, the size for which the growth and decay probabilities are equal. The size and internal energy of the critical cluster, for different values of the temperature and chemical potential, are used together with the nucleation theorems to predict the behavior of the nucleation rate as a function of these parameters. Our results agree with those found in the literature, and roughly correspond to the predictions of classical theory. In contrast to most other simulation studies, we are able to concentrate on the properties of the clusters which are most important to the process of nucleation, namely those around the critical size. This makes our simulations computationally more efficient. © 2000 American Institute of Physics. [S0021-9606(00)50209-8]

## I. INTRODUCTION

A vapor can be described as a collection of free molecules and quasibound molecular clusters which are gaining and losing molecules at various rates. Small clusters are more likely to decay than grow, and this makes it possible to understand how a supersaturated vapor, one that is thermodynamically metastable with respect to a condensed phase, can be maintained in existence. The phase transformation is impeded since it must proceed through the formation of these relatively unstable small molecular clusters. However, the ratio of growth to decay probability, per unit time, increases with cluster size. Viewing the clusters as tiny versions of continuum droplets in thermal equilibrium, the size dependence of the growth and decay probabilities is easily understood. There is competition between the free energy cost of creating the droplet–vapor interface, and the bulk reduction in free energy afforded by the phase transformation. For the so-called critical size, the probabilities of growth and decay are equal. Since growth and decay are stochastic, an individual cluster can reach the critical size through improbable sequences of molecular acquisitions. The formation of critical clusters is key to the phenomenon of nucleation, where droplets appear from a supersaturated vapor. This common but inadequately understood phenomenon has been a subject of numerous theoretical studies, aimed at interpreting the growing body of experimental data.

The underlying problem in simulating the dynamics of nucleation is that the events leading to cluster growth in a supersaturated vapor are very rare. It is therefore rather difficult to gather enough statistics by observing the spontaneous creation of critical clusters in a computer simulation of a sample of vapor. With computers becoming more and more capable all the time some simulations of this type have been done: a recent example is the work of Yasuoka and

Matsumoto.<sup>1</sup> They study a system consisting of molecules of nucleating vapor under a rather large supersaturation together with carrier gas molecules in a molecular dynamics simulation. The nucleation rate is obtained directly by counting the number of clusters of different sizes formed in the course of the simulation.

But most efforts have been focused on the properties of single clusters in specified environments. The information gathered is then used within a description of the dynamics of cluster populations to predict the nucleation rate. In such a theory, the critical cluster lies at the peak of a curve of work of formation plotted against cluster size.<sup>2–4</sup> The rate of nucleation is related to the work of formation of a critical cluster. This is the difference between the free energy of the cluster, and the free energy of the same set of molecules if they were part of a homogeneous vapor phase. This in turn is related to the excess cluster free energy: the difference between the free energy of the cluster, and the free energy its molecules would contribute if they were part of a bulk condensed phase.<sup>4</sup>

Several techniques to study the properties of individual clusters, with the aim of identifying the critical cluster size and free energy, have been described in the literature (see e.g., Refs. 5–7). An early and influential attempt to calculate the work of formation of a cluster from molecular simulations was reported by Lee, Barker, and Abraham.<sup>8</sup> Starting from a high temperature quasiideal gas of molecules, for which the free energy is known, a cluster could be formed by sequences of cooling and compression, in the process monitoring the change in free energy.<sup>9,10</sup> Using a good initial estimate of the critical size, one needs in principle to consider only a few cluster sizes to identify the maximum of the cluster work of formation curve. The main drawback with this procedure is that the reference ideal gas state is far removed from the desired conditions.

In the recent literature free energy difference calculations have become more popular. Schemes have been devel-

<sup>a)</sup>On leave of absence from Department of Physics, P.O. Box 9, 00014 University of Helsinki, Finland.

oped which, in effect, evaluate the free energy difference between clusters differing in size by one molecule.<sup>11–14</sup> Calculations of this type allow a cluster to be constructed by adding one molecule to the cluster at a time. By monitoring the change in free energy upon each addition, a free energy profile from the monomer up to the critical size can be obtained. An example of this technique, working directly with the free energies, is the Bennett method.<sup>11,15</sup> The free energy difference between clusters containing  $N$  and  $N+1$  molecules is determined by calculating ensemble averages of an energy-dependent Fermi function for a system where all  $N+1$  particles are interacting fully with each other, and for a system where the interaction of the  $(N+1)$ th particle is almost turned off.

Another route to the free energy is to find the constrained size distribution of clusters using umbrella sampling. Recent examples of this kind have been presented by Kusaka *et al.*<sup>13</sup> and ten Wolde *et al.*<sup>12</sup> Kusaka *et al.* work in a grand canonical ensemble, restricting the number of molecules to a narrow interval between  $N_l$  and  $N_u$ , and comparing the frequencies of occurrence of  $N$  molecules in the system. This gives the probability for an  $N$ -cluster to exist at a specified temperature and chemical potential, which in turn gives the cluster work of formation.

ten Wolde *et al.*<sup>12</sup> perform constant NPT simulations, and bias the sampling by adding a fictitious potential, which depends on cluster size, to the true intermolecular potential. This allows them to enhance significantly the formation of clusters within a certain size range. The effect of the additional potential is canceled when interpreting the results. The simulation yields the size distribution of the clusters, which is again closely related to the cluster free energy as a function of size. Thermodynamic integration methods are used to extend the results at one vapor pressure to other pressures.

In all these methods the critical size is identified as the size where the work of formation has its maximum. The critical work of formation can be used to evaluate the nucleation rate. If the external parameters are changed, then a repeated calculation, or alternatively thermodynamic integration,<sup>12</sup> is necessary to obtain a new free energy profile, a new critical size, and a critical work of formation.

The approaches where the full free energy profile is obtained by simulations are illustrated by the upper loop of the flow diagram shown in Fig. 1. The main effort required is the  $M$  cluster comparisons needed to establish the profile of free energy against size, where  $M$  is of the order of the critical size.

Our major aim in this article is to demonstrate how rates of nucleation of droplets from a supersaturated vapor can be calculated more efficiently from atomistic simulations, making use of two recently derived theoretical results known as the nucleation theorems.<sup>16,17</sup> The nucleation theorems have been used to extract information about critical clusters from experimental data.<sup>4,17</sup> These theorems state that if we know the size and the internal energy of the critical cluster we know how the nucleation rate changes with temperature and supersaturation. The size and energy of the critical cluster can be obtained by studying a narrow size region, with only  $m$  comparisons between clusters around the expected critical

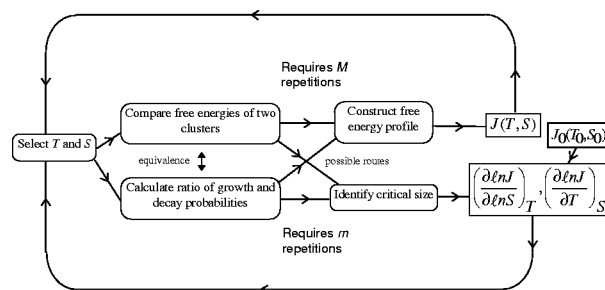


FIG. 1. Flow diagram for methods for calculating nucleation rates. Some recent schemes follow the upper loop, while our new approach is illustrated by the lower loop.  $M$  is greater than  $m$ , since in the lower loop we need to study only a narrow range of sizes, whereas in the upper loop the full size spectrum from monomers up to critical size has to be studied. The lower loop does not yield the nucleation rate, only its temperature and supersaturation derivatives: a reference rate  $J_0(T_0, S_0)$  has to be obtained by one circuit around the upper loop, for example.

size. The study of the whole size spectrum from monomers upwards is avoided, since we do not need the free energy of the critical cluster. The drawback is that we need a reference rate at one temperature and supersaturation to predict the values of nucleation rates. The reference rate can be obtained with one full free energy profile study. The procedure is illustrated in the lower loop of the flow diagram in Fig. 1. The expensive part of the calculation in the lower loop involves  $m$  repetitions, where  $m$  is smaller than  $M$ .

We have developed a novel Monte Carlo simulation technique to obtain the critical cluster information. Having tested the method for the case of new phase nucleation in the Ising model of interacting spins,<sup>18</sup> we have gone on to calculate the averaged growth and decay probabilities for clusters of Lennard-Jones atoms in a grand canonical ensemble. To enhance statistics, we actually obtain the averages of grand canonical growth and decay probabilities within a canonical scheme. The method bears some similarity to the schemes that calculate free energy differences as described above. We identify the critical cluster as the size for which the growth and decay probabilities are equal, and then exploit the nucleation theorems to determine the variation in nucleation rate as the conditions are changed. We take the necessary reference nucleation rates from the literature.

The free energy differences are associated with the probabilities of gain or loss of a molecule from the cluster when the cluster population approximates to thermal equilibrium. Our simulation method could be used to generate full free energy profiles, and the other simulation methods could be used to obtain the critical size without constructing the whole free energy profile. The idea behind the approaches where thermodynamic integration is used to obtain free energy profiles in other conditions, when the profile is known in one reference state, is very similar to the usage of nucleation theorems. The computational cost of these methods also corresponds to that of the lower loop.

The theory underlying our simulation scheme is described in the next section, and further computational details are discussed in Sec. III. The models for the equilibrium properties of Lennard-Jones fluid which we use when comparing our results with those given by the classical nucle-

ation theory are reviewed in Sec. IV, and then the nucleation theorems are described and developed in Sec. V. The critical cluster information and the nucleation rates obtained by exploiting nucleation theorems are presented in Sec. VI. Finally, we give our conclusions in Sec. VII.

## II. THEORETICAL BACKGROUND TO THE SIMULATION TECHNIQUE

If the Becker–Döring<sup>2</sup> rate equations for cluster population dynamics are applied to the subsaturated vapor in thermal equilibrium, the ratio of growth and decay probabilities, per unit time, of a cluster of  $N$  molecules can be related to the differences in grand potential between clusters of sizes  $N+1$ ,  $N$ , and  $N-1$ . Thus, observing the growth and decay of clusters under a grand canonical scheme would give us information about the relative stability of clusters of different sizes. By scaling up the cluster growth rates to represent a supersaturated vapor, we obtain a set of rate equations which describe nucleation, and which allow us to identify the critical size.

In the classical treatment the grand canonical partition function of a system of  $N$  indistinguishable particles in a volume  $V$  reads<sup>19,20</sup>

$$\Xi = \sum_{N=0}^{\infty} \frac{\gamma^N Z^N}{N!} \int_V \prod_{i=1}^N d\mathbf{r}_i \exp\left[\frac{-U_N(\{\mathbf{r}_i\})}{kT}\right], \quad (1)$$

where  $\mathbf{r}_i$  is the position of particle  $i$  and  $U_N(\{\mathbf{r}_i\})$  is the interaction energy of the  $N$ -particle system, which depends on the configuration  $\{\mathbf{r}_i\}$ . The brackets represent the set of  $N$  particle positions. Activity is defined as  $Z = \exp[\mu/(kT)]$ ,  $T$  is the temperature,  $k$  is the Boltzmann constant,  $\mu$  is the chemical potential,  $\gamma = 1/\Lambda^3$ , and  $\Lambda = \sqrt{h^2/(2\pi mkT)}$  is the thermal de Broglie wavelength of the particles. Here  $m$  is the mass of the particle and  $h$  is Planck's constant.

To be able to compare the probabilities of occurrence in the ensemble of states with different numbers of particles, we introduce  $N_{\max}$  as an upper limit for the number of particles in the system. Now the partition function can be written as

$$\Xi = \sum_{N=0}^{N_{\max}} \int_V \prod_{i=1}^{N_{\max}} d\mathbf{r}_i \frac{\gamma^N Z^N}{V^{N_{\max}-N} N!} \exp\left[\frac{-U_N(\{\mathbf{r}_i\})}{kT}\right]. \quad (2)$$

This form is obtained by inserting  $N_{\max}-N$  distinguishable noninteracting particles into the system. The factor  $V^{N_{\max}-N}$

in the denominator cancels the extra  $N_{\max}-N$  integrals over the spatial coordinates of a noninteracting particle. For a simulation to be realistic  $N_{\max}$  has to be large to make the noninteracting particles fill the space densely.

The transformation from Eq. (1) to (2) is necessary to give two systems with different number of particles a common measure: in Eq. (2) each term in the sum contains the same number of integrations, and the integrands are therefore directly related to the statistical weight of the configuration. The probability for the system to be in a state with  $N$  particles having coordinates  $\{\mathbf{r}_i\}$ , and  $N_{\max}-N$  noninteracting particles at arbitrary positions, can then be identified as

$$P(N, \{\mathbf{r}_i\}) = \frac{\gamma^N Z^N}{V^{N_{\max}-N} N!} \exp\left[\frac{-U_N(\{\mathbf{r}_i\})}{kT}\right]. \quad (3)$$

In the algorithm for grand canonical simulation presented by Yao *et al.*,<sup>21</sup> a simulation step consists of randomly choosing to try either a creation, annihilation, or movement of a particle, which is then accepted with the following probabilities.<sup>19,21</sup> We regard the act of creation to be the transformation of a noninteracting particle into a fully interacting one. The probability that one particle is created at position  $\mathbf{r}_k$  is given by  $\min[1, C(N, \{\mathbf{r}_i\} \oplus \mathbf{r}_k)]$ , where

$$\begin{aligned} C(N, \{\mathbf{r}_i\} \oplus \mathbf{r}_k) &= \frac{P(N+1, \{\mathbf{r}_i\} \oplus \mathbf{r}_k)}{P(N, \{\mathbf{r}_i\})} \\ &= \frac{\gamma Z V}{N+1} \exp\left[\frac{-(U_{N+1}(\{\mathbf{r}_i\} \oplus \mathbf{r}_k) - U_N(\{\mathbf{r}_i\}))}{kT}\right], \end{aligned} \quad (4)$$

and the probability that a particle at position  $\mathbf{r}_j$  annihilates is  $\min[1, A(N, \{\mathbf{r}_i\} \ominus \mathbf{r}_j)]$ , where  $A(N, \{\mathbf{r}_i\} \ominus \mathbf{r}_j)$  is given by

$$\begin{aligned} A(N, \{\mathbf{r}_i\} \ominus \mathbf{r}_j) &= \frac{P(N-1, \{\mathbf{r}_i\} \ominus \mathbf{r}_j)}{P(N, \{\mathbf{r}_i\})} \\ &= \frac{N}{\gamma Z V} \exp\left[\frac{-(U_{N-1}(\{\mathbf{r}_i\} \ominus \mathbf{r}_j) - U_N(\{\mathbf{r}_i\}))}{kT}\right]. \end{aligned} \quad (5)$$

The probability that a particle at position  $\mathbf{r}_j$  moves to position  $\mathbf{r}'_j$  is  $\min[1, M(N, \{\mathbf{r}_i\}, \mathbf{r}_j \rightarrow \mathbf{r}'_j)]$ , where

$$M(N, \{\mathbf{r}_i\}, \mathbf{r}_j \rightarrow \mathbf{r}'_j) = \exp\left[\frac{-(U_N(\{\mathbf{r}_1, \dots, \mathbf{r}'_j, \dots, \mathbf{r}_N\}) - U_N(\{\mathbf{r}_1, \dots, \mathbf{r}_j, \dots, \mathbf{r}_N\}))}{kT}\right]. \quad (6)$$

In order to produce a series of configurations representative of the grand canonical ensemble, the relative probabilities of attempted creation,  $\alpha_C$ , and destruction,  $\alpha_D$ , have to be equal, but the relative probability of an attempted move  $\alpha_M$  can be chosen independently. The most common choice is to set all these probabilities equal,<sup>22</sup> so  $\alpha_C = \alpha_D = \alpha_M = 1/3$ .

It is worth mentioning that the approach of Rowley *et al.*<sup>23</sup> is equivalent to the one presented here: their fictitious particles correspond to our  $N_{\max}-N$  creation sites. The difference in their formulas is due to the fact that instead of our three types of steps (move, annihilation, and creation) their grand canonical algorithm consists of two types of step: an attempted move, or an attempted change of type of a ran-

domly picked particle. In the latter case, if a real particle is picked annihilation is attempted, and if a fictitious particle is picked creation is attempted.

We introduce a cluster definition (defined in detail in the next section) and study a single cluster, i.e., configurations that violate the single cluster condition are not permitted. Thus, the actual probability for a move to be accepted is  $\delta_{\text{clu}} \min[1, M(N, \{\mathbf{r}_i, \mathbf{r}_j \rightarrow \mathbf{r}'_j\})]$ , where  $\delta_{\text{clu}} = 1$  if the cluster condition is satisfied in the new configuration, and 0 otherwise. In the same way, the creation and annihilation probabilities are subject to the cluster condition.

We could let the cluster evolve according to the grand canonical scheme, changing its shape and size (number of component particles) freely, and register the growth and decay events as a function of the cluster size to obtain the desired growth and decay probabilities. However, in this scheme the size of the cluster varies uncontrollably, and it is hard to gather the required statistics near the critical size, which by its very nature is visited infrequently.

We follow the ideas of our earlier work with the Ising model,<sup>18</sup> and study a single cluster of a particular size, changing its configuration according to the canonical scheme. We evaluate the canonical ensemble averages of the grand canonical growth and decay probabilities per Monte Carlo step, and also the ensemble average of the interaction energy of the cluster. In this way we get exactly the same information about growth and decay as we would get from true grand canonical simulations, but are able to study a specified cluster size to a desired accuracy.

The probability that annihilation is attempted within a Monte Carlo step is  $\alpha_D$ , and since the target particle is chosen at random from the real particles available, the probability of picking a particle at position  $\mathbf{r}_j$  is  $1/N$ . For configuration  $\{\mathbf{r}_i\}$  the decay rate, that is the total probability for a particle to annihilate in a Monte Carlo step, is given by

$$D(\{\mathbf{r}_i\}) = \frac{\alpha_D}{N} \sum_{j=1}^N \delta_{\text{clu}} \min[1, A(N, \{\mathbf{r}_i\} \ominus \mathbf{r}_j)], \quad (7)$$

where  $\delta_{\text{clu}}$  sets the probability to zero if the annihilation would result in splitting the cluster.

To evaluate the growth rate we take Eq. (2) to mean that there are  $N_{\text{max}} - N$  possible creation sites at random positions within the system. The probability of attempted creation is  $\alpha_C = \alpha_D$ , and that of trying the creation at position  $\mathbf{r}_k$  is  $1/(N_{\text{max}} - N)$ . The total creation rate is the sum of the probabilities to create a particle at any of the  $N_{\text{max}} - N$  positions. Thus, the creation rate for a configuration  $\{\mathbf{r}_i\}$  reads

$$G(\{\mathbf{r}_i\}) = \frac{\alpha_C}{N_{\text{max}} - N} \sum_{k=1}^{N_{\text{max}} - N} \delta_{\text{clu}} \min[1, C(N, \{\mathbf{r}_i\} \oplus \mathbf{r}_k)], \quad (8)$$

where  $\delta_{\text{clu}}$  is zero if the particle created would not be part of the cluster according to the cluster definition.

The growth rate is essentially the average of growth probabilities over  $N_{\text{max}} - N$  sites, and it is independent of  $N_{\text{max}}$  if  $N_{\text{max}}$  is large enough to provide sufficient sampling. Both growth and decay rate depend on the volume of the system  $V$  in a complex way due to the minimum

function employed, but their ratio is independent of  $V$ . This can be seen, for example, in the limit  $V \rightarrow \infty$ . In this limit the following inequalities always hold:  $A(N, \{\mathbf{r}_i\} \ominus \mathbf{r}_j) < 1$  and  $C(N, \{\mathbf{r}_i\} \oplus \mathbf{r}_k) > 1$ . If we denote the volume of the part of space where creation is allowed, according to the cluster condition, by  $V_C$ , we get  $G(\{\mathbf{r}_i\}) = \alpha_C V_C / V$  for the growth rate and  $D(\{\mathbf{r}_i\}) = \alpha_D N / (\gamma ZV) \exp[-(U_{N-1}(\{\mathbf{r}_i\} \ominus \mathbf{r}_j) - U_N(\{\mathbf{r}_i\})) / (kT)]$  for the decay rate. It is clearly seen that the ratio of  $G$  to  $D$  does not depend on  $V$ .

We evaluate the ensemble averages  $D \equiv \langle D \rangle_{\text{can}}$  and  $G \equiv \langle G \rangle_{\text{can}}$  for different sizes, and identify the critical size as the size for which these averages are equal. Then we obtain an accurate ensemble average for the energy  $\langle E \rangle$  of this single size.

### III. COMPUTATIONAL DETAILS AND TEST CALCULATIONS

We define a cluster as a connected network of neighbors, and two particles are considered neighbors if they are less than  $r_{\text{neigh}}$  apart. This definition has been introduced by Stillinger.<sup>5</sup> The value  $r_{\text{neigh}} = 1.5\sigma$  was chosen as it corresponds to the first minimum of the radial distribution function of a liquid.<sup>12</sup>  $\sigma$  is the length scale of the Lennard-Jones potential. We compare our results with those of ten Wolde *et al.*<sup>12</sup> but unfortunately we cannot use exactly the same cluster definition as they do: in addition to requiring the cluster to be a network of neighbors, they demand that each particle in the cluster should have five neighbors to be liquid-like. In their simulation they include explicitly the vapor molecules surrounding the cluster, and these provide the necessary neighbors for the surface particles in the cluster. In our case there are no explicit vapor molecules around the cluster; thus requiring five neighbors makes the clusters extremely compact. Trial simulations showed that this would dramatically increase the critical size.

The entire system is taken to be a sphere with radius  $R$ , which is related to volume  $V$  of the system appearing in Eqs. (2), (5) by  $V = 4\pi R^3/3$ . Around the origin we set up a cluster of the size studied, which satisfies the cluster definition. Due to the cluster definition, creation can be successful only at sites which are within the distance  $r_{\text{neigh}}$  of some existing particle. This is used to reduce the computing time: we keep track of the particle that is furthest from the origin and try creation only in the origin-centered sphere with radius  $R' = r_{\text{furthest}} + r_{\text{neigh}}$ . Outside this sphere creation can never be successful. In Eq. (8) the  $N_{\text{max}} - N$  attempted creation sites cover the whole volume  $V$  with a fixed density, but  $(N_{\text{max}} - N)[1 - (R'/R)^3]$  terms of the sum are automatically zero. The radius  $R$  can be taken as very large to avoid the cluster ever being close to the boundaries of the system: the actual volume of the system enters the simulation only through Eqs. (4) and (5), and the calculation of  $N_{\text{max}}$  for Eq. (8) from the fixed density  $N_{\text{max}}/V$ . When changing the configuration, we attempt, on average, one canonical move for every particle. Every tenth configuration, the origin is moved to the new center-of-mass.

We study a sufficient number of configurations to obtain accurate ensemble averages. The accuracy is monitored by

TABLE I. Test calculations for  $N=1$  and  $N=2$  clusters with different densities of creation sites  $N_{\max}/V$  (for  $N=1$ ) and number of sample configurations  $N_{\text{config}}$  (for  $N=2$ ). Calculations are performed with the truncated and shifted Lennard-Jones potential with  $kT/\epsilon=0.741$ ,  $Z'=0.02$ , and  $R=5\sigma$ .  $\rho_l$  is the molecular density of the liquid phase. The digits after the  $\pm$  sign denote the statistical error in the two last digits of the result, e.g.  $0.020\ 10\pm 01$  means  $0.020\ 10\pm 0.000\ 01$ .

$N$	$N_{\max}/V$	$N_{\text{config}}$	$\langle G \rangle_{\text{sim}}$	$\langle G \rangle_{\text{exact}}$	$\langle D \rangle_{\text{sim}}$	$\langle D \rangle_{\text{exact}}$	$\langle E \rangle_{\text{sim}}/\epsilon$	$\langle E \rangle_{\text{exact}}/\epsilon$
1	$100\ \rho_l$	1	0.020 10±01	0.020 11	...	...	...	...
1	$1000\ \rho_l$	1	0.020 12±01	0.020 11	...	...	...	...
2	$100\ \rho_l$	1000	0.030 17±16	0.031 66	0.0791±52	0.0823	-0.70±03	-0.68
2	$100\ \rho_l$	10 000	0.030 22±06	0.031 66	0.0805±17	0.0823	-0.69±02	-0.68

comparing the averages over equal subblocks of the chain of configurations. We can study widely separated sizes with modest accuracy to locate the interesting size region, and perform more accurate simulations around the expected critical size.

The particles forming the cluster are simple Lennard-Jones atoms interacting through the potential

$$U(r_{ij}) = 4\epsilon \left[ \left( \frac{\sigma}{r_{ij}} \right)^{12} - \left( \frac{\sigma}{r_{ij}} \right)^6 \right], \quad (9)$$

where  $\epsilon$  and  $\sigma$  are the well depth and the length scale of the potential, respectively, and where  $r_{ij}$  is the separation between atoms labeled  $i$  and  $j$ .

We performed two sets of simulations: one to get the critical size as a function of chemical potential difference between vapor and liquid,  $\Delta\mu/(kT)$  (defined in detail in the beginning of Sec. IV), at a constant temperature, and the other to get the critical size as a function of temperature with constant  $\Delta\mu/(kT)$ . The first set was performed with the following truncated and shifted potential:  $U'(r_{ij})=U(r_{ij})-U(r_{\text{cutoff}})$  when  $r < r_{\text{cutoff}}$  and  $U'(r_{ij})=0$  when  $r > r_{\text{cutoff}}$ . The cutoff radius was  $r_{\text{cutoff}}=2.5\sigma$ , and no long-range corrections were used. The second set of simulations was performed with the full potential (9). The reason for using two versions of the potential is that we wanted to compare our results to those of ten Wolde *et al.*,<sup>12</sup> which are obtained at  $kT/\epsilon=0.741$  with the truncated and shifted potential, while the literature studies used for comparison at other temperatures refer to the full potential.

The parameters entering the simulation are the temperature  $T$ , and reduced activity  $Z'$  defined as

$$Z' = Z \times (\sigma/\Lambda)^3 = \exp[\mu/(kT) - 3 \ln(\Lambda/\sigma)]. \quad (10)$$

First we studied clusters consisting of one or two atoms only. For these sizes the growth and decay probabilities (the latter makes sense for the two-cluster only, and even then the cluster requirement of one neighbor has to be relaxed) can be evaluated exactly. The ensemble average of the growth rate for a ‘‘cluster’’ consisting of a single atom is given by

$$\langle G \rangle_{N=1} = \frac{1}{V} \int_0^{r_{\text{neigh}}} \min \left[ 1, \frac{Z\gamma V}{2} \exp \left( \frac{-U(r)}{kT} \right) \right] 4\pi r^2 dr, \quad (11)$$

where  $U(r)$  is the interaction energy between the existing atom at the origin and the created atom at distance  $r$  from it. From Eq. (7), the average decay rate for a dimer is

$$\langle D \rangle_{N=2} = \frac{1}{Q} \int_0^{r_{\text{neigh}}} \min \left[ 1, \frac{2}{Z\gamma V} \times \exp \left( \frac{-U(r)}{kT} \right) \right] \exp \left( \frac{-U(r)}{kT} \right) 4\pi r^2 dr, \quad (12)$$

and the average energy for the dimer is

$$\langle E \rangle_{N=2} = \frac{1}{Q} \int_0^{r_{\text{neigh}}} U(r) \exp \left( \frac{-U(r)}{kT} \right) 4\pi r^2 dr, \quad (13)$$

where  $U(r)$  is the interaction energy of two atoms which are separated by distance  $r$ ; the normalization factor is  $Q = \int_0^{r_{\text{neigh}}} \exp[-U(r)/(kT)] 4\pi r^2 dr$ , and  $\exp[-U(r)/(kT)]$  is the Boltzmann factor associated with a dimer configuration characterized by an atomic separation  $r$ .

Finally, the average growth rate for the dimer is

$$\langle G \rangle_{N=2} = \frac{1}{QV} \int_{r=0}^{r_{\text{neigh}}} \int_{x=-1.5}^{r/2} \int_{y=0}^{\sqrt{r_{\text{neigh}}^2-x^2}} \left\{ 4\pi r^2 dr \times 4\pi y dx dy \min \left[ 1, \frac{Z\gamma V}{3} \exp \left( \frac{-U(r)}{kT} \right) \right] \times \exp \left( \frac{-U_3(r,x,y)}{kT} \right) \right\}, \quad (14)$$

where the integration limits for  $x$  and  $y$  arise from the nature of the creation volume  $V_C$  which consists of two partially overlapping spheres, and depend on the separation of the two atoms in the dimer denoted by  $r$ .  $U_3(r,x,y)$  is the interaction energy of three atoms, the first one of which is situated in the origin, the second one at Cartesian coordinates  $(r,0,0)$  and the third one at  $(x,y,0)$ .

Table I shows the examples of these test calculations with  $kT/\epsilon=0.741$ ,  $Z'=0.02$ , and  $R=5\sigma$ , for the truncated and shifted potential. The simulation results agree well with the ones obtained by evaluation of the integrals in Eqs. (11) to (14) using MATHEMATICA.<sup>24</sup> Moreover, in doing this we have gained information about how many configurations have to be studied and what the value of  $N_{\max}$  should be to get enough statistics. We found that the density of the attempted creation sites ( $N_{\max}/V$ ) has to be of the order of 100 times the density of the liquid at the prevailing temperature. The number of configurations needed for accurate results naturally increases with the size of the cluster.

Our simulations were performed on a Compaq Alpha Server GS140 with a 525 MHz processor.  $N_{\max}/V=100$  was

TABLE II. Average CPU time elapsed ( $t$  in seconds) in obtaining the average growth and decay probabilities in example simulations with different densities of potential creation sites  $N_{\max}/V$  and number of sample configurations  $N_{\text{config}}$  for different size intervals  $[N_i, N_f]$ .  $\rho_l$  is the molecular density of the liquid phase.  $kT/\epsilon=0.741$ ,  $Z'=0.02$ .

$N_{\max}/V$	$N_{\text{config}}$	$t$ [1,2]	$t$ [10, 11]	$t$ [25, 26]	$t$ [69, 70]
100 $\rho_l$	1000	16	185	478	2448
100 $\rho_l$	100	1.7	17	50	318
50 $\rho_l$	100	0.9	7.4	27	142

used in all simulations, and the number of configurations per size was generally 10 000, although larger values of up to 100 000 were used occasionally for improved accuracy. To give a picture of the time required for the simulations, Table II shows times required for example simulations. It is seen that while the time required increases fairly linearly with  $N_{\max}/V$  and number of configurations, it grows nonlinearly when the size of the cluster increases. The times do not change significantly if we use the full potential instead of the truncated one. The radius of the box ( $R$ ) does not affect the times either. The simulations for the largest size we studied,  $N=75$ , took about 10 h CPU time with 10 000 configurations.

#### IV. PHYSICO-CHEMICAL DATA AND COMPARISON MATERIAL

ten Wolde *et al.*<sup>12</sup> use umbrella sampling to compute the free energy of a cluster as a function of its size, and identify the critical size as the size where the work of formation has its maximum. They report the critical sizes at constant temperature  $kT/\epsilon=0.741$  as a function of chemical potential difference  $\Delta\mu(P)=\mu(P)-\mu_l(P)$ , where  $\mu_l$  and  $\mu$  are the chemical potentials of the liquid and vapor, respectively, and  $P$  is the pressure. They use the truncated and shifted Lennard-Jones potential with  $r_{\text{cutoff}}=2.5\sigma$  and no long-range corrections. The smallest critical size they studied is around 66 and the largest 350. The critical sizes obtained from their simulations are in good agreement with classical theory,<sup>2</sup> which predicts the critical size  $N^*$  to be given by

$$N_{\text{class}}^* = \frac{32\pi\Gamma_{\infty}^3}{3\rho_l^2\Delta\mu^3}, \quad (15)$$

where  $\Gamma_{\infty}$  is the surface tension of a flat liquid/vapor interface and  $\rho_l$  is the number density of the liquid at coexistence.

We want to compare the critical sizes given by our method with classical theory, and with the results of ten Wolde *et al.* at the smallest sizes they studied. We also want to use the nucleation theorems to predict the behavior of the nucleation rate as a function of temperature and  $\Delta\mu/(kT)$ . For these purposes we have to relate the chemical potential  $\mu$  that enters our simulations to the molecular density  $\rho$  and the pressure  $P$  of the vapor, and hence to the chemical potential difference  $\Delta\mu$ .

At relatively low densities, a Lennard-Jones fluid can be described by the virial expansion truncated after the second virial coefficient  $B(T)$ :

$$P = kT\rho(1 + B\rho). \quad (16)$$

The chemical potential for a system described by this equation is given by

$$\frac{\mu}{kT} = \ln(\rho\Lambda^3) + 2B\rho. \quad (17)$$

A more accurate description is given by the following Haar-Shenker-Kohler (HSK) model:<sup>25</sup>

$$P = kT\rho \left( 1 + B\rho + \frac{\eta^2(10 - 12\eta + 4\eta^2)}{(1 - \eta)^3} \right), \quad (18)$$

$$\frac{\mu}{kT} = \ln(\rho\Lambda^3) + 2B\rho + \frac{\eta^2(15 - 21\eta + 8\eta^2)}{(1 - \eta)^3}, \quad (19)$$

where  $\eta = \pi\rho d^3/6$  and the hard sphere diameter  $d$  is

$$d = \int_0^{2^{1/6}} [1 - \exp\{- (U(r) + \epsilon)/(kT)\}] dr. \quad (20)$$

The chemical potential difference is related to the vapor pressure  $P$  by the following equation:

$$\Delta\mu(P) = \int_{P_s}^P \left[ \frac{1}{\rho(P')} - \frac{1}{\rho_l} \right] dP', \quad (21)$$

where the liquid is assumed incompressible.

ten Wolde kindly provided us with data for vapor density  $\rho$  as a function of pressure  $P$ , obtained from their simulations with the truncated and shifted potential for pressures in the range  $0.007 \leq P\sigma^3/\epsilon \leq 0.017$  at temperature  $kT/\epsilon=0.741$ . We found that the Lennard-Jones fluid, under their simulation conditions, can be described by the virial equation of state (16), and the second virial coefficient was found to be  $B/\sigma^3 = -7.506$ . The behavior of the vapor clearly differs from that of an ideal gas. The higher-order term in Eq. (18) is not needed to obtain a good fit to the data. ten Wolde *et al.*<sup>12</sup> also present the value for the saturation vapor pressure  $P_s\sigma^3/\epsilon=0.00783$ , and the necessary values for surface tension and liquid density needed in Eq. (15):  $\Gamma_{\infty}\sigma^2/\epsilon=0.494$  and  $\rho_l\sigma^3=0.766$ .

For temperatures other than  $kT/\epsilon=0.741$  we found neither critical size data nor nucleation rates for comparison. Comparisons at other temperatures are thus made with classical theory only. But the required physico-chemical data found in the literature refer to the full potential, and for this reason the full potential is used in our simulations for temperatures  $kT/\epsilon=0.70$ ,  $kT/\epsilon=0.75$ , and  $kT/\epsilon=0.80$ . Lotfi *et al.*<sup>26</sup> report that the HSK equations (18), (19) can be applied to the Lennard-Jones systems at these temperatures. They also give the saturation vapor pressure  $P_s$ , saturation vapor density  $\rho(P_s)$ , equilibrium chemical potential  $\mu_s$ , the latent heat of evaporation per atom  $L$ , and the average interaction energy per atom in the liquid  $e_l$  at these temperatures. An estimate for the surface tension at these temperatures is obtained by fitting a second-order polynomial to the data given by Mecke *et al.*<sup>27</sup> The second virial coefficients obtained by integrating the Mayer  $f$ -function are tabulated in the book by Hirschfelder *et al.*<sup>28</sup> Table III summarizes the values used in this work.

TABLE III. Physico-chemical data for the full potential Lennard-Jones fluid. Apart from the virial coefficient, the results are obtained from simulations with the truncated potentials (using varying cut-off distances), adding long-range corrections. The reduced chemical potential is defined as  $\mu_s^* = \mu_s/(kT) - 3 \ln \Lambda/\sigma$ .

$kT/\epsilon$	$P_s\sigma^3/\epsilon$	$\rho(P_s)\sigma^3$	$\mu_s^*$	$B/\sigma^3$	$d/\sigma$	$\rho_l\sigma^3$	$\Gamma_\infty\sigma^2/\epsilon$	$L/\epsilon$	$e_l/\epsilon$
0.70	0.001 31	0.001 93	-6.298	-9.8647	1.028 14	0.842 66	1.1452	6.758	-6.0957
0.75	0.002 64	0.003 63	0.690	-8.7460	1.025 79	0.821 58	1.0301	6.5899	0.9069
0.80	0.004 70	0.006 17	0.184	-7.8209	1.023 57	0.799 29	0.918 23	6.4018	0.7102

### V. NUCLEATION THEOREMS

Now let us establish the form of the nucleation theorems that can be used to interpret our simulation results. The derivation of nucleation theorems presented by Ford<sup>4</sup> involves an unusual definition of saturation ratio  $S' = \rho_1/\rho_1^s$ , where  $\rho_1$  and  $\rho_1^s(T)$  are the monomer number concentrations in the supersaturated and saturated vapor, respectively. For an ideal gas this reduces to the standard definition  $S = P/P_s$ ,  $P$  and  $P_s$  being the pressures of supersaturated and saturated vapor, respectively. With these definitions the first nucleation theorem reads

$$\left(\frac{\partial \ln J}{\partial \ln S'}\right)_T = 1 + N^*, \quad (22)$$

where  $J$  is the nucleation rate and  $N^*$  is the size (number of molecules) of the critical cluster. The second nucleation theorem (neglecting terms of the order of  $\rho/\rho_l$  or smaller) is given by

$$\left(\frac{\partial \ln J}{\partial T}\right)_{\ln S'} = \frac{1}{kT^2}[L - kT + E_x(N^*)], \quad (23)$$

where  $L$  is the latent heat per molecule in the vapor-liquid transition, and  $E_x(N^*) = E(N^*) - N^*e_l(T)$  is the excess internal energy of the cluster (compared to bulk liquid at pressure  $P$ ), which is loosely related to the surface energy of the cluster. Both of the theorems are valid for a nonideal as well as an ideal vapor.

To convert the first theorem to an appropriate form for this study we write

$$\begin{aligned} \left(\frac{\partial \ln J}{\partial \ln S'}\right)_T &= \left(\frac{\partial \ln J}{\partial \Delta\mu/(kT)}\right)_T \left(\frac{\partial \Delta\mu/(kT)}{\partial P}\right)_T \left(\frac{\partial P}{\partial \rho}\right)_T \\ &\times \left(\frac{\partial \rho}{\partial \ln S'}\right)_T. \end{aligned} \quad (24)$$

The second derivative on the right-hand side can be evaluated using Eq. (21) and the third derivative using the equation of state. The last derivative is evaluated assuming that the deviations from ideal gas law arise from the presence of dimers in addition to the dominant monomers in the vapor. For the case where temperature is kept constant and the critical size is evaluated as a function of  $\Delta\mu/(kT)$  we use the virial equation of state (16). The second virial coefficient and the number of dimers in the vapor can be related by assuming that  $\rho = \rho_1 + 2\rho_2$  and  $P/(kT) = \rho_1 + \rho_2$  which leads to

$-B = \rho_2/\rho^2$  and  $\rho_1 = \rho + 2B\rho^2$ , where  $\rho_2$  is the number concentration of dimers. We obtain the following form for the first theorem

$$\left(\frac{\partial \ln J}{\partial \Delta\mu/(kT)}\right)_T = (1 + N^*) \left(1 - \frac{\rho}{\rho_l}\right) (1 + \mathcal{O}(B\rho)^2). \quad (25)$$

It should be noted that Oxtoby and Kashchiev<sup>16</sup> presented the first nucleation theorem in the form

$$\left(\frac{\partial W^*}{\partial \mu}\right)_T = N^*, \quad (26)$$

where  $W^*$  is the work of formation of a critical cluster. This form is exact and free of the corrections described above, which arise largely from taking the partial derivative with respect to  $\Delta\mu$  and not  $\mu$ .

In the set of simulations where  $\Delta\mu/(kT)$  is kept constant, and the critical cluster size and energy are found as a function of temperature, we use the HSK Eq. (18). To reformulate the second nucleation theorem, we notice that since we are again going to neglect terms smaller than  $B\rho$ , we can work with Eq. (16) instead of Eq. (18), since the  $\eta$ -dependent term in Eq. (18) is small compared to the  $B\rho$  term. Starting from the identity

$$\left(\frac{\partial \ln J}{\partial T}\right)_{\Delta\mu/kT} = \left(\frac{\partial \ln J}{\partial T}\right)_{S'} + \left(\frac{\partial \ln J}{\partial \ln S'}\right)_T \left(\frac{\partial \ln S'}{\partial T}\right)_{\Delta\mu/kT}, \quad (27)$$

and using relation (21) and the relations between  $\rho$ ,  $B$ , and  $\rho_l$  presented above Eq. (25), we get the following form for the second nucleation theorem:

$$\begin{aligned} \left(\frac{\partial \ln J}{\partial T}\right)_{\Delta\mu/kT} &= \frac{1}{kT^2}[L - kT + E_x(N^*)] + (N^* + 1) \left(\frac{\rho}{\rho(P_s)} - 1\right) \\ &\times \left(\frac{P_s}{kT^2\rho_l} + \frac{P_s}{kT\rho_l^2} \frac{\partial \rho_l}{\partial T} - \frac{L}{\Delta v kT^2\rho_l}\right). \end{aligned} \quad (28)$$

We have also neglected terms of the order of  $\rho/\rho_l$  or smaller, since this was done when deriving Eq. (23). The Clausius-Clapeyron equation  $\partial P_s/\partial T = L/(T\Delta v)$  has been used to express the derivative of the vapor pressure in terms of the molecular latent heat  $L$  and the difference of molecular volumes  $\Delta v = 1/\rho(P_s) - 1/\rho_l$ .

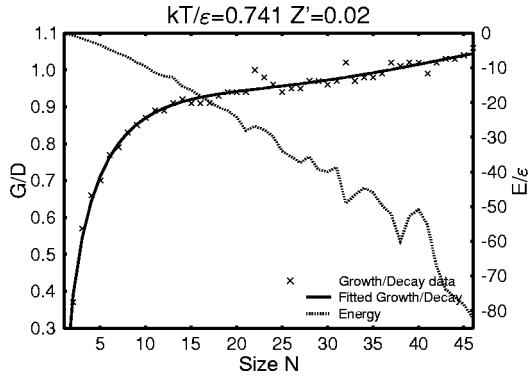


FIG. 2. The ratio of average growth rate to average decay rate, and the average energy as a function of size for Lennard-Jones clusters. Results are computed with the truncated and shifted potential.

In the next section, we compare the nucleation rates obtained using the nucleation theorems with the classical expression for the nucleation rate<sup>2,29,30</sup> (modified by a factor  $1/S$ ):

$$J_{\text{class}} = \sqrt{\frac{2\Gamma_{\infty} \rho_1^2}{\pi m S \rho_l}} \exp\left(\frac{-16\pi\Gamma_{\infty}^3}{3kT\rho_l^2\Delta\mu^2}\right), \quad (29)$$

where  $\rho_1$  is again the concentration of monomers in the vapor, assumed to be given by the virial approximation  $\rho_1 = \rho + 2B\rho^2$ .

## VI. RESULTS

### A. Critical size as a function of chemical potential

Figure 2 shows the results of a set of simulations for  $Z' = 0.02$ , corresponding to  $\Delta\mu/(kT) = 0.702$ , for the truncated and shifted potential. The smooth curve fitted to the  $G/D$  data indicates that the critical size is about 37. The energy starts to fluctuate at larger sizes due to insufficient statistics. If a more accurate estimate for the critical cluster energy is needed, it can be obtained with extended simulations for this size only.

Figure 3 shows the critical size and critical cluster energy as a function of the reduced activity  $Z'$ . The uncertainty

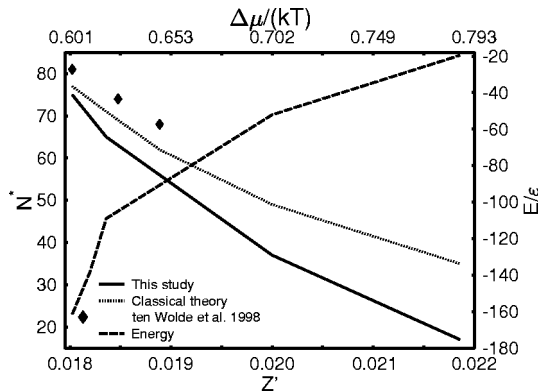


FIG. 3. The critical size and the average internal energy of the critical cluster as a function of reduced activity (or chemical potential). The temperature is  $kT/\epsilon = 0.741$ . Results are computed with the truncated and shifted Lennard-Jones potential.

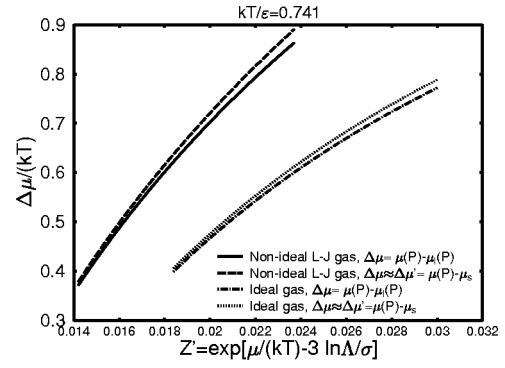


FIG. 4. The connection between the chemical potential difference that drives the nucleation, and the reduced activity for a Lennard-Jones fluid in different approximations.  $\mu$  and  $\mu_l$  are the chemical potentials of the vapor and liquid phases, respectively, and  $\mu_s$  is the chemical potential at phase equilibrium.

in the critical size is less than or equal to  $\pm 1$ . The results of our simulations are compared with the results of ten Wolde *et al.*,<sup>12</sup> as well as with classical theory predictions. The connection between  $Z'$  and  $\Delta\mu/(kT)$  is obtained using Eqs. (16) and (17) together with Eqs. (10) and (21). Figure 4 shows  $\Delta\mu/(kT)$  as a function of reduced activity in different approximations. It is seen that neglecting the  $1/\rho_l$  term in Eq. (21), resulting in the often-used approximation  $\Delta\mu \approx \Delta\mu' = \mu - \mu_s$ , does not make a big difference, but the nonideal behavior of the Lennard-Jones gas is significant. This has been recently pointed out also by Senger *et al.*<sup>10</sup>

We obtain fairly good agreement with the lowest critical sizes studied by ten Wolde *et al.*, bearing in mind that our cluster definition is rather different from theirs. The classical theory (where cluster definition is not specified) agrees quite well with both sets of simulation results, lying between them. For small sizes, the classical results start to deviate from the results of our simulations, giving consistently larger critical sizes. This is no surprise, since the capillarity approximation used in classical theory is expected to fail for small cluster sizes. We cannot increase  $Z'$  much further than we have, since we reach the spinodal at  $Z' = 0.0245$  or  $P = 3.15P_s$  according to Eq. (16). The highest pressure studied at this temperature is  $P = 2.63P_s$ .

### B. Nucleation rate as a function of chemical potential

The first nucleation theorem (25) can be used to obtain the nucleation rate as a function of  $\Delta\mu$  at constant temperature, once the rate  $J_0$  is known for one value  $\Delta\mu_0/(kT)$ , and if we know the critical size and the density as a function of  $\Delta\mu$ :

$$\ln J = \ln J_0 + \int_{\Delta\mu_0/(kT)}^{\Delta\mu/(kT)} (1 + N^*) \left(1 - \frac{\rho}{\rho_l}\right) d[\Delta\mu/(kT)], \quad (30)$$

where  $N^*$  depends on  $\Delta\mu/(kT)$ .

For the reference rate,  $J_0$ , we use a value reported in the literature. In another recent article, ten Wolde *et al.*<sup>29</sup> have used molecular dynamics to calculate the nucleation rate for the same Lennard-Jones system at the temperature  $kT/\epsilon = 0.741$  for one saturation ratio  $S = P/P_s = 1.53$ , which cor-

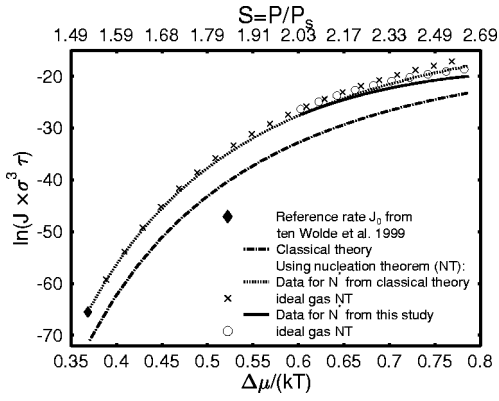


FIG. 5. The nucleation rate as a function of the chemical potential difference. The temperature is  $kT/\epsilon=0.741$ . Results are computed with the truncated and shifted Lennard-Jones potential. The lines show the rate obtained using the full form of the first nucleation theorem with classical critical size (dotted line) and the critical sizes given by our simulations (solid line). The crosses and circles show the corresponding result obtained using the first nucleation theorem derived in the ideal gas approximation.

responds to  $\Delta\mu_0/(kT)=0.37$ . The value of the nucleation rate is  $J_0=3.5\times 10^{-29}/(\sigma^3\tau)$ , where  $\tau=\sigma^{-1}\sqrt{m\sigma^2/\epsilon}$  is the time unit, and  $m$  is the mass of the Lennard-Jones atom. This supersaturation is well below the range we consider, and thus we use classical values for the critical size, together with Eq. (30), to extrapolate this reference rate up to  $\Delta\mu/(kT)=0.60$ , which is the lowest value of chemical potential we studied. This is justified since the simulations of ten Wolde *et al.*<sup>12</sup> indicate that the classical predictions for the critical size are satisfactory at this temperature for  $0.37\leq\Delta\mu/(kT)\leq 0.65$ . We then use the critical sizes obtained from our simulations to extrapolate the nucleation rate further, into the interval  $0.60\leq\Delta\mu/(kT)\leq 0.79$ , which corresponds to  $0.018\leq Z'\leq 0.022$  and  $2.03\leq S\leq 2.66$ .

Figure 5 shows the comparison between nucleation rates obtained using Eqs. (30) and (29). We also show that using  $N_{class}^*$  in Eq. (30) for  $0.60\leq\Delta\mu/(kT)\leq 0.79$  results in a nucleation rate curve with the same slope as the classical curve, as it should. The effect of the nonideality correction  $1-\rho/\rho_l$  in Eq. (25) is also demonstrated. The nonideality correction to the first nucleation theorem is small but not completely insignificant.

### C. Critical size and average interaction energy as a function of temperature

We performed simulations at temperatures  $kT/\epsilon=0.70, 0.75$ , and  $0.80$  at a constant  $\Delta\mu/(kT)=1.39305$ . The relation between  $Z'$  and  $\Delta\mu/(kT)$  is given by Eqs. (18) and (19) together with Eqs. (10) and (21) using parameters listed in Table III. Table IV shows the simulation conditions as well as the results for the critical size and average interaction energy of the critical cluster. The simulation conditions are closest to the spinodal at  $kT/\epsilon=0.8$  where the vapor density in the simulation is  $\rho\sigma^3=0.05124$  while the spinodal density is  $\rho\sigma^3\approx 0.067$ . We have evaluated the classical value for the critical size using Eq. (15). At  $kT/\epsilon=0.70$  and  $kT/\epsilon$

TABLE IV. Simulation parameters and results for critical size and critical cluster interaction energy, different temperatures with  $\Delta\mu/(kT)=1.39305$  kept constant. Classical predictions for size  $N_{cla}^*$  are also shown.

$kT/\epsilon$	$\rho\sigma^3$	$S$	$Z'$	$N_{sim}^*$	$N_{cla}^*$	$\langle E(N^*) \rangle_{sim}$
0.70	0.008996	4.38	0.00753848	82	76	-243.6 $\epsilon$
0.75	0.019594	4.62	0.0139343	46	48	-153.3 $\epsilon$
0.80	0.05124	5.30	0.0232905	10	29	-9.613 $\epsilon$

$=0.75$  the classical theory gives reasonably good estimates for the simulation results, but at  $kT/\epsilon=0.80$  the classical theory starts to fail badly.

The parameters shown in Table III, and used to obtain classical predictions, have been obtained with the truncated potential using long range corrections. The values given do not represent the system accurately, especially for the surface tension. This can be seen from the results of Mecke *et al.*<sup>27</sup> which change when changing the cut-off radius from  $5\sigma$  to  $6.5\sigma$ , the latter being the highest value they used. Thus, the difference between the simulation results and the classical predictions is a combination of classical approximations and inaccurate data.

### D. Nucleation rate as a function of temperature

If we know the nucleation rate  $J_0$  for one temperature  $T_0$ , we can obtain the temperature dependence of the rate by integrating the second nucleation theorem (28):

$$\ln J = \ln J_0 + \int_{T_0}^T \left( \frac{\partial \ln J}{\partial T} \right)_{\Delta\mu/(kT)} dT. \quad (31)$$

We use the classical nucleation rate  $J_0=J_{class}(kT_0/\epsilon=0.7, \Delta\mu_0/(kT_0)=1.39305)$  as a reference rate, due to the lack of a suitable simulation result for the nucleation rate for the full potential.

Figure 6 shows the logarithm of the nucleation rate as a function of temperature. We compare the classical prediction with the results obtained when using the full Eq. (28) and when neglecting the nonideality correction. The correction is found to be small but noticeable. Nucleation theorems only give the slope of the curve, and it agrees with the slope of the

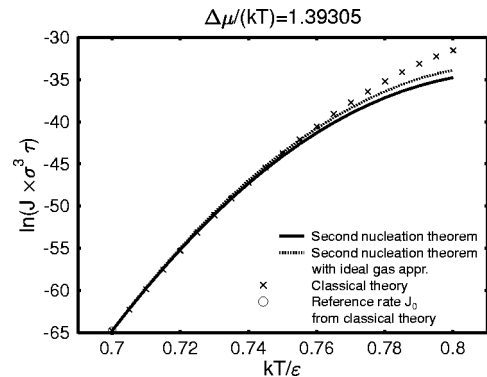


FIG. 6. The nucleation rate as a function of the temperature. Results are computed with full Lennard-Jones potential. The classical nucleation rate at  $kT/\epsilon=0.7$  is used as the reference rate in the method based on nucleation theorems.

classical curve up to temperatures  $kT/\epsilon=0.75$ . At  $kT/\epsilon=0.80$  where the critical size deviates from the classical value significantly, the slopes are significantly different.

## VII. CONCLUSIONS

We have presented a new technique for obtaining the relative probabilities for the growth and decay of molecular clusters in a vapor. We have done this by evaluating the canonical ensemble averages of grand canonical growth and decay probabilities, per Monte Carlo step, for clusters of Lennard-Jones atoms, as a function of the cluster size. The growth and decay probabilities are related to the differences in free energy between clusters. Despite the multitude of techniques described in the literature, we chose to develop the present growth and decay simulation since we feel it is physically more transparent and straightforward to apply. The size for which growth and decay probabilities are equal is identified as the critical size: the cluster with the maximum work of formation. For Lennard-Jones atoms the critical sizes obtained using our method are consistent with literature values and classical theory predictions.

We use the critical cluster size and energy, together with two nucleation theorems, to determine the behavior of the droplet nucleation rate when the temperature and vapor supersaturation are changed. This same approach was demonstrated for the Ising system in our previous article.<sup>18</sup> Using the nucleation theorems relieves us of the need to know the free energy of the critical cluster. This can save computational effort: to obtain the free energy one has to create the critical cluster step by step from a state whose free energy is known. This could involve many calculations for clusters of various sizes, and perhaps for a range of conditions. In contrast, we can focus our simulation only on sizes around the critical size. The price paid is that we then only know the derivatives of the nucleation rate, and need a reference case to predict the absolute value of the nucleation rate. We use literature values for the reference rate. Of course, critical cluster properties could be obtained by any method which compares the free energies, or relative populations, of clusters in a vapor, and the information could be fed into the nucleation theorems in the way we have described.

We have derived corrections to the nucleation theorems due to the nonideal nature of the vapor phase, and found that these corrections are numerically small for the Lennard-Jones system under the conditions studied. However, the connection between  $\mu$  and  $\Delta\mu$  is significantly affected by the nonideality of the vapor. We have extrapolated nucleation rates calculated for one set of conditions to other temperatures and vapor supersaturations. The dependence of the nucleation rate so obtained agrees fairly well with classical values for nucleation rates, and as expected the deviation increases as the critical cluster size gets smaller, and as the conditions approach the spinodal limit.

The simulation method and analysis can be extended to more complicated systems, for example molecules such as water, and multicomponent clusters. Also, the cluster definition we used can be easily modified. Our method has proved to be an effective way to gather information about nucleating clusters. We have therefore demonstrated the power of nucleation theorems in the analysis of molecular simulations.

## ACKNOWLEDGMENTS

The authors thank I. Kusaka for providing us with a grand canonical Monte Carlo code, which was used as a starting point in the development of our code. Thanks are due to P. R. ten Wolde for giving us the additional pressure–density data for Lennard-Jones vapor. We thank the Center for Scientific Computing (CSC) in Espoo, Finland for computer time. The work was funded by the U.K. Engineering and Physical Sciences Research Council under Grant GR/L78499 and by the Academy of Finland under Project No. 64314.

- <sup>1</sup>K. Yasuoka and M. Matsumoto, *J. Chem. Phys.* **109**, 8451 (1998).
- <sup>2</sup>R. Becker and W. Döring, *Ann. Phys. (Leipzig)* **24**, 719 (1935).
- <sup>3</sup>F. F. Abraham, *Homogeneous Nucleation Theory* (Academic, New York, 1974).
- <sup>4</sup>I. J. Ford, *Phys. Rev. E* **56**, 5615 (1997).
- <sup>5</sup>F. H. Stillinger, *J. Chem. Phys.* **38**, 1486 (1963).
- <sup>6</sup>D. Zhukhovitskii, *J. Chem. Phys.* **103**, 9401 (1995).
- <sup>7</sup>R. B. McClurg and R. Flagan, *J. Chem. Phys.* **105**, 7648 (1996).
- <sup>8</sup>J. K. Lee, J. A. Barker, and F. F. Abraham, *J. Chem. Phys.* **58**, 3166 (1973).
- <sup>9</sup>B. Senger, P. Schaaf, D. S. Corti, R. Bowles, J.-C. Voegel, and H. Reiss, *J. Chem. Phys.* **110**, 6421 (1999).
- <sup>10</sup>B. Senger, P. Schaaf, D. S. Corti, R. Bowles, D. Pointu, J.-C. Voegel, and H. Reiss, *J. Chem. Phys.* **110**, 6438 (1999).
- <sup>11</sup>B. N. Hale, *Aust. J. Phys.* **49**, 425 (1996).
- <sup>12</sup>P. R. ten Wolde and D. Frenkel, *J. Chem. Phys.* **109**, 9901 (1998).
- <sup>13</sup>I. Kusaka, Z.-G. Wang, and J. Seinfeld, *J. Chem. Phys.* **108**, 6829 (1998).
- <sup>14</sup>K. Oh and X. Zeng, *J. Chem. Phys.* **110**, 4471 (1999).
- <sup>15</sup>B. N. Hale and R. Ward, *J. Stat. Phys.* **28**, 487 (1982).
- <sup>16</sup>D. W. Oxtoby and D. Kashchiev, *J. Chem. Phys.* **100**, 7665 (1994).
- <sup>17</sup>I. J. Ford, *J. Chem. Phys.* **105**, 8324 (1996).
- <sup>18</sup>H. Vehkamäki and I. J. Ford, *Phys. Rev. E* **59**, 6483 (1999).
- <sup>19</sup>D. Heermann, *Computer Simulation Methods in Theoretical Physics* (Springer-Verlag, Berlin, 1986).
- <sup>20</sup>G. K. Schenter, S. Kathmann, and B. Garrett, *J. Chem. Phys.* **110**, 7951 (1999).
- <sup>21</sup>J. Yao, R. Greenkorn, and C. Chao, *Mol. Phys.* **46**, 587 (1982).
- <sup>22</sup>M. P. Allen and D. J. Tildesley, *Computer Simulations of Liquids* (Clarendon, Oxford, 1987).
- <sup>23</sup>L. A. Rowley, D. Nicholson, and N. Parsonage, *J. Comput. Phys.* **17**, 401 (1975).
- <sup>24</sup>MATHEMATICA, Version 3.0 for Linux, Wolfram Research, Inc., Copyright 1988-96.
- <sup>25</sup>J. Fischer and M. Bohn, *Mol. Phys.* **58**, 395 (1986).
- <sup>26</sup>A. Lotfi, J. Vrabec, and J. Fischer, *Mol. Phys.* **76**, 1319 (1992).
- <sup>27</sup>M. Mecke and W. Winkelmann, *J. Chem. Phys.* **107**, 9264 (1997).
- <sup>28</sup>J. Hirschfelder, C. F. Curtiss, and R. Bird, *Molecular Theory of Gases and Liquids* (Wiley, New York, 1964).
- <sup>29</sup>P. R. ten Wolde, M. J. Ruiz-Montero, and D. Frenkel, *J. Chem. Phys.* **110**, 1591 (1999).
- <sup>30</sup>J. Zeldovich, *Sov. Phys. JETP* **12**, 525 (1942).